Chapter 3
Classical Results

This chapter is devoted to classical results, mostly presented in the pioneer works by Mikhail Lidov and Yoshihide Kozai. To start with, we derive the secular Lidov-Kozai Hamiltonian (the LK Hamiltonian) for the circular R3BP, where the averaged perturbation is approximated by the quadrupole term of the Hamiltonian expansion in the ratio of semimajor axes of the test particle (tertiary) and the gravitating binary. Since there is only one angular variable remaining in the LK Hamiltonian (the argument of pericenter), the corresponding motion equations can be solved by quadrature. The fact that the second angle (the longitude of the ascending node) is missing is a lucky fortuitous property of the problem.

Kozai proposed a convenient technique to analyze the qualitative properties of these secular effects: he constructed phase portraits, characterizing the secular evolution of the eccentricity and the argument of pericenter for various initial conditions. Taking into account that the corresponding phase trajectories lie on the level curves of the LK Hamiltonian, the trajectories can be drawn without integration of the motion equations. The topology of the phase portraits depends essentially on the norm of the vertical component of the tertiary's orbital angular momentum. At its certain value, a bifurcation occurs: whereas for the norm's greater values the argument of pericenter always circulates, for its smaller values an equilibrium point appears, accompanied with the trajectories (around the point), corresponding to libration of the argument of pericenter. This libration island is nothing but the famous *Lidov-Kozai resonance*.

The integration of the averaged motion equations by quadrature requires application of elliptic functions. Already in 1962 Kozai demonstrated how this could be done (Kozai 1962), but only quite a considerable time later on his ideas were realized by Lidov's disciple Mikhail Vashkovyak (1999) and Kinoshita and Nakai (1999, 2007).

I. I. Shevchenko, *The Lidov-Kozai Effect – Applications in Exoplanet Research and Dynamical Astronomy*, Astrophysics and Space Science Library 441,
DOI 10.1007/978-3-319-43522-0_3

To complete our review of the classical results, we discuss how the LKE can be suppressed in various dynamical situations. Indeed, if an additional perturbation dominates over the LK-term in the Hamiltonian of the motion, then the LKE may disappear (Lidov 1963b; Morbidelli 2002). In particular, such a suppression explains the stable existence of the *regular* satellites of Uranus. In their case, the suppression "agent" is the satellites' orbital precession forced by the Uranus oblateness and the moons' mutual perturbations.

3.1 A Single-Averaged R3BP

As an example of a secular theory, we consider Moiseev's scheme of averaging of the R3BP. The reason is that this scheme is useful for our further analysis, as it has a direct relation to the LK scheme. Indeed, a double-averaging is utilized in the LK scheme, thus involving the single-averaging as an ingredient of the whole procedure.

In the single-averaged R3BP, the perturbing function is averaged over one variable (that with the largest frequency of variation), namely, the mean anomaly of the satellite. As soon as a perturber is in an outer orbit, the satellite's mean anomaly is "faster" than that of the perturber. In the Hill approximation, only the lowest order term in the ratio of the semimajor axes of the satellite and the perturber is taken into account in the perturbing function. This averaging scheme was introduced by Moiseev (1945a,b).[1]

Moiseev (1945a,b) deduced equations of motion in the single-averaged problem and found two integrals of the motion. Contrary to the double-averaged case (considered in this book later on), there is no third integral here; thus, the problem is not integrable in the spatial case (when the system has three degrees of freedom).

Based on Moiseev's averaging scheme, Vashkovyak (2005) derived explicit equations of motion in the single-averaged R3BP, in the Hill approximation. Here we reproduce these equations in convenient notations, and, following Vashkovyak (2005), delineate the conditions for their applicability.

Consider the motion of a planetary satellite perturbed by a distant external body (e.g., the Sun). The perturbing body is assumed to move in a circular orbit of radius $a_{\rm pert}$. The planetocentric Keplerian orbital elements of the satellite, i.e., the semimajor axis, eccentricity, inclination, argument of pericenter, longitude of ascending node, and mean anomaly, are denoted, as usually, by a, e, i, ω, Ω, and M, respectively. The angles are referred to the plane of motion of the perturbing body and to a fixed arbitrary direction in this plane.

[1] Nikolay Dmitrievich Moiseev (1902–1955), a professor of the Moscow University, was the founder of the Moscow school of celestial mechanics. The mentioned papers were typeset in 1941, but, due to calamities of the war, the publication was delayed until 1945.

The Keplerian mean motion of the satellite is $n = (\mathcal{G}m)^{1/2}/a^{3/2}$, and that of the perturbing body is $n_{\rm pert} = [\mathcal{G}(m_0 + m_{\rm pert})]^{1/2}/a_{\rm pert}^{3/2}$. Following Vashkovyak (2005), we introduce a dimensionless parameter of the problem, $\nu = n_{\rm pert}/(n\beta)$, where $\beta = 3m_{\rm pert}a^3/(16m_0a_{\rm pert}^3)$. $\mathcal{G}$ is the gravitational constant, m_0 and $m_{\rm pert}$ are the masses of the primary (planet) and the perturbing body, respectively. If $m_0/m_{\rm pert} \ll 1$, then $n_{\rm pert}^2 \approx \mathcal{G}m_{\rm pert}/a_{\rm pert}^3$, $\beta \approx 3n_{\rm pert}^2/(16n^2)$, and $\nu \approx 16n/(3n_{\rm pert})$.

The unitless "time" is defined as

$$\tau = \beta n(t - t_0), \tag{3.1}$$

where t_0 is the initial time.

The mean longitude of the perturbing body is given by

$$\lambda_{\rm pert} = \lambda_{\rm pert}|_{t=t_0} + n_{\rm pert}(t - t_0) = \lambda_{\rm pert}|_{\tau=0} + \nu\tau. \tag{3.2}$$

The longitude of ascending node of the satellite's orbit, Ω, is present in the averaged perturbing function R only in combination with the mean longitude of the perturbing body, $\lambda_{\rm pert}$.[2] Denoting

$$\Upsilon = \Omega - \lambda_{\rm pert}|_{\tau=0} - \nu\tau, \tag{3.3}$$

let us average the perturbing function $\mathcal{R}$ (corresponding to the third term in expression (2.14); see also Murray and Dermott 1999) over the mean anomaly of the satellite:

$$\mathcal{V} = \frac{1}{2\pi}\int_0^{2\pi} \mathcal{R}\,{\rm d}M. \tag{3.4}$$

Here the perturbing function is normalized by factor $\mathcal{G}m\beta/a$. Taking the integral in the quadrupole (Hill) approximation, one has

$$\mathcal{V} = \mathcal{V}_{\rm H} + O(a/a_{\rm pert})^3, \tag{3.5}$$

where

$$\begin{aligned}\mathcal{V}_{\rm H} = {} & \frac{4}{3} + 2(e^2 - \sin^2 i) + e^2\sin^2 i(5\cos 2\omega - 3) - 10e^2\cos i\sin 2\omega\sin 2\Upsilon + \\ & + [2\sin^2 i + 10e^2\cos 2\omega + e^2\sin^2 i(3 - 5\cos 2\omega)]\cos 2\Upsilon\end{aligned} \tag{3.6}$$

[2]This follows from the so-called D'Alembert rules, specifying which combinations of angles can be present in the Fourier expansions of perturbing functions. The formulation of the D'Alembert rules is given in section 1.9.3 in Morbidelli (2002).

(Vashkovyak 2005). The equations of motion are easily derivable, as soon as a perturbing function is given (see Murray and Dermott 1999). In accord with expression (3.6), the secular equations for the single-averaged Hill problem are given by

$$\frac{\mathrm{d}a}{\mathrm{d}\tau} = 0, \tag{3.7}$$

$$\frac{\mathrm{d}e}{\mathrm{d}\tau} = 10e(1-e^2)^{1/2}[\sin^2 i \sin 2\omega + (2-\sin^2 i)\sin 2\omega \cos 2\Upsilon + 2\cos i \cos 2\omega \sin 2\Upsilon], \tag{3.8}$$

$$\frac{\mathrm{d}i}{\mathrm{d}\tau} = -2\sin i\,(1-e^2)^{-1/2}\{5e^2 \cos i \sin 2\omega(1-\cos 2\Upsilon) - \\ -[2+e^2(3+5\cos 2\omega)]\sin 2\Upsilon\}, \tag{3.9}$$

$$\frac{\mathrm{d}\omega}{\mathrm{d}\tau} = 2(1-e^2)^{-1/2} \times \\ \times\{4+e^2-5\sin^2 i + 5(\sin^2 i - e^2)\cos 2\omega + 5(e^2-2)\cos i \sin 2\omega \sin 2\Upsilon + \\ +[5(2-e^2-\sin^2 i)\cos 2\omega - 2 - 3e^2 + 5\sin^2 i]\cos 2\Upsilon\}, \tag{3.10}$$

$$\frac{\mathrm{d}\Upsilon}{\mathrm{d}\tau} = -\nu - 2(1-e^2)^{-1/2}\{[2+e^2(3-5\cos 2\omega)]\cos i\,(1-\cos 2\Upsilon) - 5e^2 \sin 2\omega \sin 2\Upsilon\}. \tag{3.11}$$

Moiseev (1945b) found out that the secular system in this problem has two integrals:

$$a = \text{const}, \tag{3.12}$$

$$\mathcal{V} + \nu(1-e^2)^{1/2}\cos i = \text{const}. \tag{3.13}$$

In the Hill approximation, $\mathcal{V} = \mathcal{V}_\mathrm{H}$, where $\mathcal{V}_\mathrm{H}$ is given by formula (3.6).

Vashkovyak (2005) formulated conditions for the applicability of the secular equations to describe the long-term motion of natural satellites of planets in the Solar system. Let us enumerate them. Recall first of all that the radius of a planet's Hill sphere a_H, in units of the semimajor axis of a perturbing body, a_pert, is given by

$$a_\mathrm{H}/a_\mathrm{pert} = \left[3\left(1+\frac{m_\mathrm{pert}}{m_0}\right)\right]^{-1/3}. \tag{3.14}$$

Then, the semimajor axis of a satellite's orbit, a, in units of $a_{\rm H}$, is equal to

$$\frac{a}{a_{\rm H}} = 4\left[\frac{4}{3\nu^2}\left(1+\frac{m_0}{m_{\rm pert}}\right)^2\right]^{1/3} \approx 2^{8/3}3^{-1/3}\nu^{-2/3} \approx 4.40\nu^{-2/3}. \tag{3.15}$$

The planetocentric orbit of a satellite should lie within the Hill sphere. This implies the inequality $a(1+e) \lesssim a_{\rm H}$. Therefore, an allowed lower limit for ν is given by $\nu_{\rm min} \approx 9.24$ at $e = 0$, and by $\nu_{\rm min} \approx 26.1$ at $e = 1$.

Vashkovyak (2005) compared these theoretical bounds with the values of ν observed for the real planetary satellites in the Solar system. For the real satellites (including the irregular most distant satellites of the giant planets), the ratio of mean motions, $n_{\rm pert}/n$, does not exceed ≈ 0.16; therefore, one has $\nu \approx 16n/(3n_{\rm pert}) \gtrsim 33$, and the theoretical condition for $\nu_{\rm min}$ is thus satisfied.

3.2 The Double-Averaged R3BP

The first secular theory in celestial mechanics was constructed by Lagrange and Laplace: they built an analytical theory describing the long-term averaged behaviour of the Solar system planets. However, this theory was limited to the case of small mass parameters and small planetary eccentricities and inclinations; besides, resonances were assumed to be absent. Brown (1936) applied techniques of canonical transformations to describe the long-term averaged behaviour of stellar triple systems; in particular, he obtained the Hamiltonian in the quadrupole approximation. Three integrals in the double-averaged circular R3BP were found by Moiseev (1945a,b).

3.2.1 The Lidov-Kozai Hamiltonian

In this subsection, we derive the secular Lidov-Kozai Hamiltonian (the LK Hamiltonian) for the circular R3BP, where the averaged perturbation is approximated by the quadrupole term of the Hamiltonian expansion in the ratio of semimajor axes of the test particle (tertiary) and the gravitating binary. Since there is only one angular variable that remains in the LK Hamiltonian (the argument of pericenter), the corresponding motion equations can be solved by quadrature.

In the *restricted* version of the N-body problem, one of the bodies (called the *test particle* or simply the *particle*) is massless in the sense that it gravitates only passively: the particle's motion is affected by the gravity of all other bodies, but the particle's gravity does not affect the motion of other bodies. The orbits of the massive bodies are assumed to be known. According to expression (2.14), the

Hamiltonian is given by

$$\mathcal{H} = \mathcal{H}_{\text{Kepler}} + \mathcal{H}_{\text{interaction}} \tag{3.16}$$

(Malhotra 2012; Murray and Dermott 1999), where the *Keplerian Hamiltonian* is

$$\mathcal{H}_{\text{Kepler}} = -\frac{\mathcal{G}m_0}{2a} \tag{3.17}$$

(where a is the semimajor axis of the particle's orbit around primary m_0), and the *interaction Hamiltonian* is

$$\mathcal{H}_{\text{interaction}} = -\sum_{i=1}^{N} \mathcal{G}m_i \left[\frac{1}{\|\mathbf{r} - \mathbf{r}_i\|} - \frac{(\mathbf{r} - \mathbf{r}_0) \cdot (\mathbf{r}_i - \mathbf{r}_0)}{\|\mathbf{r}_i - \mathbf{r}_0\|^3} \right], \tag{3.18}$$

where $\mathbf{r}$ is the position vector of the test particle.

In the R3BP, the interaction Hamiltonian reduces to

$$\mathcal{H}_{\text{interaction}} = -\mathcal{G}m_1 \left[\frac{1}{\|\mathbf{r} - \mathbf{r}_1\|} - \frac{(\mathbf{r} - \mathbf{r}_0) \cdot (\mathbf{r}_1 - \mathbf{r}_0)}{\|\mathbf{r}_1 - \mathbf{r}_0\|^3} \right]. \tag{3.19}$$

Let us derive the Lidov-Kozai Hamiltonian in the R3BP, taking expression (3.19) as a starting point. For this purpose, we follow an approach by Malhotra (2012).

As there remains only one perturber, further on we designate m_1 as m_{pert}. Thus, the masses of the primary and the perturber are designated by m_0 and m_{pert}; the radius of perturber's circular orbit by a_{pert}; the semimajor axis of particle's orbit by a. It is assumed that $a \ll a_{\text{pert}}$.

Setting $\mathbf{r}_0 = 0$, we rewrite Equation (3.19) in the form

$$\mathcal{H}_{\text{interaction}} = -\mathcal{G}m_{\text{pert}} \left(\frac{1}{\|\mathbf{r} - \mathbf{r}_{\text{pert}}\|} - \frac{\mathbf{r} \cdot \mathbf{r}_{\text{pert}}}{\|\mathbf{r}_{\text{pert}}\|^3} \right), \tag{3.20}$$

where $\mathbf{r}$ and $\mathbf{r}_{\text{pert}}$ are the *astrocentric* position vectors of the particle and the perturber, respectively.

After expanding Equation (3.20) in power series of ratios $\|\mathbf{r}\| / \|\mathbf{r}_{\text{pert}}\|$ up to the second order, the double-averaging over the angles (both the mean longitude of the perturber and the mean longitude of the particle) is performed. In the process, the variables are transformed to the osculating orbital elements. (The perturber's orbital plane is chosen to be the reference plane, with respect to which the particle's inclination is measured.)

The averaging can be performed either by straightforward integration over the angles (see, e.g. Broucke 2003), or by application of the normalization methods described in Sects. 2.6 and 2.7, e.g., the von Zeipel method, as accomplished by

Kozai (1962). To the given (quadrupole) order of the perturbation theory, the resulting double-averaged Hamiltonian will be the same, whatever approach is chosen, and is given by

$$\langle \mathcal{H}_{\text{interaction}} \rangle \simeq -\frac{\mathcal{G}m_{\text{pert}}a^2}{8a_{\text{pert}}^3}\left[2+3e^2-3(1-e^2+5e^2\sin^2\omega)\sin^2 i\right], \tag{3.21}$$

where ω is the particle's argument of pericenter. Of course, all the orbital elements of the particle's orbit in this formula are the transformed (*averaged*) ones (though the notations are the same as for the original osculating elements).

From expression (3.21), it immediately follows that there exist three independent integrals of motion. First of all, the Hamiltonian $\langle \mathcal{H}_{\text{interaction}} \rangle$ is time independent; thus, it is an integral. Besides, $\langle \mathcal{H}_{\text{interaction}} \rangle$ is independent of the mean longitude l and the longitude of ascending node Ω; therefore, the conjugate Delaunay momenta $L = [\mathcal{G}(m_0 + m_{\text{pert}})a]^{1/2}$ and $H = L(1-e^2)^{1/2}\cos i$ (see definitions (2.15)) are also integrals. We find that our three-degree-of-freedom averaged system has three integrals and thus is completely integrable.

Note that the Delaunay momentum $G = L(1-e^2)^{1/2}$ is not conserved; thus, the eccentricity varies secularly, and so does the inclination; these variations are coupled due to the conservation of H.

The three integrals can be rewritten in the classical form:

$$c_0 \equiv a = \text{const}, \tag{3.22}$$

$$c_1 \equiv (1-e^2)\cos^2 i = \text{const}, \tag{3.23}$$

$$c_2 \equiv e^2\left(\frac{2}{5}-\sin^2 i\sin^2\omega\right) = \text{const} \tag{3.24}$$

(Kozai 1962; Lidov 1961). The expression for c_2 is derived from the equalities $\langle \mathcal{H}_{\text{interaction}} \rangle = \text{const}$ and $H = \text{const}$.

Expressed in terms of the Delaunay variables (see Sect. 2.4), the Hamiltonian $\langle \mathcal{H}_{\text{interaction}} \rangle$ takes the form

$$\langle \mathcal{H}_{\text{interaction}} \rangle = -\frac{\mathcal{G}m_{\text{pert}}a^2}{8a_{\text{pert}}^3}\left[5+3\frac{H^2}{L^2}-6\frac{G^2}{L^2}-15\left(1-\frac{G^2}{L^2}-\frac{H^2}{G^2}+\frac{H^2}{L^2}\right)\sin^2\omega\right]. \tag{3.25}$$

This is the *Lidov-Kozai Hamiltonian*, expressed explicitly in canonical variables (Malhotra 2012). (In literature on the subject, it is more customary to find the Hamiltonian expressed in orbital elements, as presented in Equation (3.21); then, to derive the corresponding equations of motion one must rewrite the Hamiltonian in canonical variables first.)

The corresponding Hamiltonian equations are given by

$$\dot{G} = -\frac{\partial \mathcal{H}}{\partial \omega} = -\frac{15\mathcal{G}m_{\text{pert}}a^2}{8a_{\text{pert}}^3} e^2 \sin^2 i \sin 2\omega \,, \tag{3.26}$$

$$\dot{\omega} = \frac{\partial \mathcal{H}}{\partial G} = \frac{3\mathcal{G}m_{\text{pert}}a^2}{4a_{\text{pert}}^3 G} \left[2\frac{G^2}{L^2} + 5\left(\frac{H^2}{G^2} - \frac{G^2}{L^2} \right) \sin^2 \omega \right], \tag{3.27}$$

$$\dot{\Omega} = \frac{\partial \mathcal{H}}{\partial H} = -\frac{3\mathcal{G}m_{\text{pert}}a^2}{4a_{\text{pert}}^3} \frac{H}{L^2} \left[1 - 5\left(1 - \frac{L^2}{G^2} \right) \sin^2 \omega \right]. \tag{3.28}$$

The exact LK-resonance takes place, if $\dot{\omega} = 0$. From Equation (3.27) it follows that, apart from some limiting situations, the condition is satisfied at $\omega = \pm\pi/2$ and $G = (5H^2L^2/3)^{1/4}$. Thus, the LK-resonance center is situated at $\omega = \pm\pi/2$, $e = [1-(5c_1/3)^{1/2}]^{1/2}$, $i = \arccos(3c_1/5)^{1/4}$. This stationary solution exists if $c_1 \leq 3/5$. Accordingly, the *critical inclination*, above which the LK-resonance exists, is given by $i_{\text{crit}} \approx 39.2°$.

3.2.2 Equations and Constants of Motion

We still consider the motion of a massless particle in the framework of the R3BP. The perturber's orbit is set to be circular of radius a_{pert}; its plane defines the reference plane. Let us write down the particle's equations of secular motion in the Keplerian elements (a, e, i, ω, Ω). Though designated in the same way as the ordinary osculating Keplerian elements, it is implied that they are *mean*, representing the time averages on the timescales of the orbital periods of the particle and the perturber.

In the double-averaged Equations (3.26), (3.27) and (3.28), one may transform the Delaunay variables to the Keplerian elements, and, thus, obtain the equations of motion in the elements. Alternatively, averaging Equations (3.7), (3.8), (3.9), (3.10) and (3.11) with respect to the perturber's mean anomaly (see Broucke 2003; Lidov 1961), and returning to non-normalized time t, one gets the same resulting equations:

$$\frac{\mathrm{d}a}{\mathrm{d}t} = 0, \tag{3.29}$$

$$\frac{\mathrm{d}e}{\mathrm{d}t} = \frac{15}{8} \frac{n_{\text{pert}}^2}{n} e(1-e^2)^{1/2} \sin^2 i \sin 2\omega, \tag{3.30}$$

$$\frac{\mathrm{d}i}{\mathrm{d}t} = -\frac{15}{16} \frac{n_{\text{pert}}^2}{n} e^2(1-e^2)^{-1/2} \sin 2i \sin 2\omega, \tag{3.31}$$

$$\frac{\mathrm{d}\omega}{\mathrm{d}t} = \frac{3}{8}\frac{n_{\mathrm{pert}}^2}{n}(1-e^2)^{-1/2}[(5\cos^2 i - 1 + e^2) + 5(1-e^2-\cos^2 i)\cos\omega], \tag{3.32}$$

$$\frac{\mathrm{d}\Omega}{\mathrm{d}t} = \frac{3}{8}\frac{n_{\mathrm{pert}}^2}{n}\cos i(1-e^2)^{-1/2}[5e^2\cos 2\omega - 3e^2 - 2], \tag{3.33}$$

where n_{pert} is the mean motion of the perturbing body.

These equations of motion in the elements are nothing but the Lagrange equations (see Murray and Dermott 1999) defined by the double-averaged perturbing function. The equations of motion in the elements $(a, e, i, \omega, \Omega)$ in the double-averaged R3BP are considered in a number of papers; see, e.g., Innanen et al. (1997), Carruba et al. (2002), and Tamayo et al. (2013). Corrections to the first two papers are given in Carruba et al. (2003).

The single-averaged problem (described by Equations (3.7), (3.8), (3.9), (3.10) and (3.11)) has a *cylindrical symmetry* with respect to the z axis: the perturber's mean anomaly M_{pert} is present in the equations only through the difference $D = \Omega - M_{\mathrm{pert}}$. This entails the absence of Ω in the right-hand sides of the equations in the double-averaged problem; this absence is obvious in Equations (3.29), (3.30), (3.31), (3.32) and (3.33). The mean anomaly M is also eliminated from the right-hand sides, due to the averaging. Only three elements (e, i, and ω) remain present.

We see that equations (3.30), (3.31), and (3.32) form a self-contained closed system of equations, the semimajor axis a being constant. Once they are solved, the longitude of the ascending node Ω can be immediately found from Equation (3.33).

Though the mean anomaly M is averaged out, an equation for the mean anomaly at epoch M_0 is still warranted. It is given by

$$\frac{\mathrm{d}M_0}{\mathrm{d}t} = -\frac{1}{8}\mathcal{G}m_{\mathrm{pert}}\frac{n_{\mathrm{pert}}^2}{n}[(3e^2+7)(3\cos^2 i - 1) + 15(1+e^2)\sin^2 i\cos^2\omega]. \tag{3.34}$$

It can be used to define an approximate mean anomaly, $M = M_0 + nt$, if needed. The formula for M is so simple only because $a = \mathrm{const}$ and $n = \mathrm{const}$ here. Note that the semimajor axis a is constant both in the single-averaged and double-averaged problems.

Equations (3.30)–(3.31) give an integral:

$$c_1 = (1-e^2)\cos^2 i, \tag{3.35}$$

which is essentially the z component of the angular momentum squared. Obviously, $0 \le c_1 \le 1$. Besides, the constancy of (3.35) means that (1) the secular variations of e and i are coupled in anti-phase if $0 \le i \le \pi/2$ (in particular, if i decreases tending to zero, $i \to 0$, then e increases, $e \to (1-c_1)^{1/2}$), and (2) the variations of e and i are coupled in phase if $\pi/2 \le i \le \pi$ (in particular, if i increases tending to π, $i \to \pi$, then e increases as well, $e \to (1-c_1)^{1/2}$).

The averaged perturbing function (or, the averaged interaction potential, see Equation (3.21)) is constant, because it does not contain time explicitly. Simplifying Equation (3.21) by using Equation (3.35), one has one more non-trivial integral:

$$c_2 = e^2 \left(\frac{2}{5} - \sin^2 i \sin^2 \omega \right). \tag{3.36}$$

Quite obviously, $-3/5 \le c_2 \le -2/5$ (because $0 \le (\sin i \sin \omega)^2 \le 1$).

The conserved semimajor axis a, integral c_1, and integral c_2 form a set of three integrals of the double-averaged problem; thus, this averaged problem, which has three degrees of freedom, is completely integrable.

Recall that the single-averaged problem is non-integrable (as discussed in Sect. 3.1), as the original non-averaged one.

3.2.3 *Classification of Orbits*

A straightforward analysis of analytical expressions for c_1 and c_2, performed by Lidov (1961), allowed him to locate the domains of possible motion in the (c_1, c_2) plane.

In Fig. 3.1, it is the "triangle" ABEDA. The classification of dynamical regimes, according to location in this triangle in the (c_1, c_2) plane, is discussed in a number of works, in particular, see Lidov (1961) and Broucke (2003).

Inside the triangle, the vertical line $c_2 = 0$ separates two basic types of motion: (1) at $c_2 < 0$ the orbits have the argument of pericenter librating; (2) at $c_2 > 0$ the

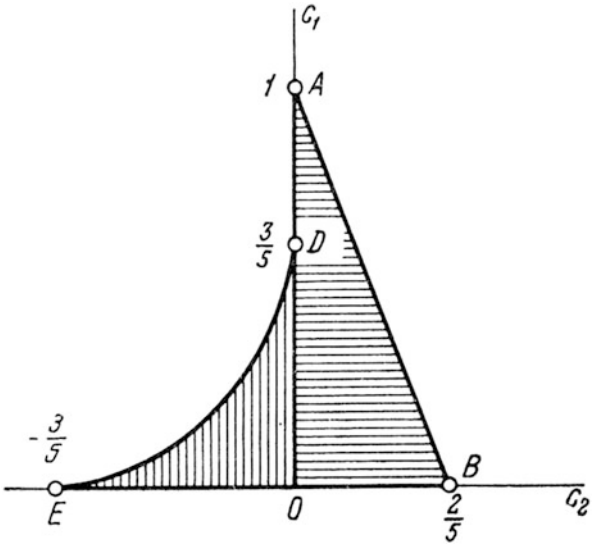

Fig. 3.1 The domains of possible values of constants c_1 and c_2 (Figure 1 from Lidov 1961)

orbits have the argument of pericenter circulating.[3] In case (1), the libration of ω takes place around either $\pi/2$ or $3\pi/2$. The librating orbits exist only if $0 \le c_1 \le 3/5$. In case (2), the circulating orbits exist in the whole interval $0 \le c_1 \le 1$.

The triangular region ABEDA in Fig. 3.1 has three corners (A, B, E) and two other important boundary points more (D and 0, i.e., the zero point). The corner points A, B, and E have the following dynamical meaning.

Point A ($c_1 = 1$, $c_2 = 0$) corresponds to the circular equatorial orbit ($e = 0$, $\sin i = 0$).

Point B ($c_1 = 0$, $c_2 = \frac{2}{5}$) corresponds to the rectilinear orbits ($e = 1$) with an arbitrary inclination and $\sin\omega = 0$.

Point E ($c_1 = 0$, $c_2 = -\frac{3}{5}$) corresponds to the polar orbits ($\cos i = 0$) with an arbitrary eccentricity and ω such that $e^2(5\sin^2\omega - 2) = 3$. At $e = 1$ one has a rectilinear orbit with $\sin\omega = \pm 1$.

The points D and 0 have the following dynamical meaning.

Point D ($c_1 = \frac{3}{5}$, $c_2 = 0$) corresponds to the circular ($e = 0$) orbits with a *critical inclination*. The critical inclination is defined by the equation $\cos^2 i = \frac{3}{5}$; therefore, $i_{\text{crit}} \approx 39.23°$.[4] The point D is a bifurcation point (that is why the inclination is called critical): on decreasing the values of c_1, the orbits with librating pericenter (those with $c_2 < 0$) emerge just at this point, at $c_1 = \frac{3}{5}$. In other words, the *LK-resonance* becomes possible.

Point 0 ($c_1 = c_2 = 0$) corresponds to the orbits of the following three kinds:

1. circular ($e = 0$) polar ($\cos i = 0$) orbits with arbitrary ω;
2. elliptic (e arbitrary) polar ($\cos i = 0$) orbits with $\sin^2\omega = \frac{2}{5}$;
3. inclined (i arbitrary) rectilinear ($e = 1$) orbits with $\sin^2 i \sin^2\omega = \frac{2}{5}$.

The boundary segments AB, BE, ED, and DA of the triangle ABEDA have the following dynamical meaning.

Segment AB corresponds to the orbits such that $2c_1 + 5c_2 = 2$. Taking c_1 and c_2 from Equations (3.35) and (3.36), one has

$$(5e^2\sin^2\omega + 2 - 2e^2)\sin^2 i = 0. \tag{3.37}$$

The first factor is zero only at point B, where $e = 1$ and $\sin\omega = 0$ simultaneously. Thus, apart from point B, the whole segment is defined by the second factor in Equation (3.37), which is zero at the inclinations $i = 0$ and $i = \pi$. The corresponding orbits are the equatorial planar orbits, with eccentricity $e = (1 - c_1)^{1/2}$; these orbits are precessing, namely, ω increases.

[3] The vertical line $c_2 = 0$ is analogous, in such a way, to the separatrix of the nonlinear mathematical pendulum: it separates the regimes of librations and circulations of an angle.

[4] Note that this value is the critical inclination in the considered model. If the problem is non-hierarchical (say, as in a real asteroid–Jupiter–Sun system), or the body which the particle orbits is oblate (say, as in a real satellite–planet–Sun system), the critical inclinations would be different.

Interval BE corresponds to the orbits such that $c_1 = 0$. This condition corresponds either to the polar ($\cos i = 0$) or to the rectilinear ($e = 1$) orbits.

Curve ED corresponds to the orbits such that the elements e and i are constant.[5] The constant values are related by the equation $e^2 = 1 - \frac{5}{2}\cos^2 i$; whereas $\omega = \pm\pi/2$. These equilibrium solutions correspond to the centers of the LK-resonance.

Interval DA ($c_2 = 0$, $3/5 < c_1 < 1$) corresponds to the orbits such that $e = 0$, i.e., to the circular orbits.

Interval 0D ($c_2 = 0$, $c_1 < 3/5$) corresponds to the separatrix solutions,[6] separating the domains of librating and circulating arguments of pericenter. On the separatrices, the eccentricity e tends either to zero or away from it. For these orbits, the relation $\sin^2 i \sin^2 \omega = \frac{2}{5}$ holds.

The orbits inclined above the critical value $i_{\rm crit} = \arccos(3/5)^{1/2}$ may suffer large eccentricity variations, especially large if an orbit is close to the separatrix of the LK-resonance. The reason is that the LK-resonance is present in the phase space if $i > i_{\rm crit}$. In case of the 90°-inclination the eccentricity always tends to unity, no matter what is its initial value; thus, the pericentric distance tends to zero, and such (polar) orbits are practically short-lived.

What is more, the value $\arccos(3/5)^{1/2} \approx 39°$ for the critical inclination $i_{\rm crit}$ is valid only in the limit $a/a_{\rm pert} \to 0$ (where a and $a_{\rm pert}$ are the semimajor axes of the particle and the perturber, respectively). As soon as, in any real problem, $a/a_{\rm pert}$ is not zero, $i_{\rm crit}$ is less than the classical value. The critical inclination diminishes with increasing $a/a_{\rm pert}$. This was shown already by Kozai (1962) both numerically and analytically: e.g., if $a/a_{\rm pert} = 0.5$ then $i_{\rm crit} \approx 32°$, as follows from figure 1 in Kozai (1962).

If $c_1 = (1-e^2)^{1/2}\cos i$ is close to unity, the particle's eccentricity and inclination suffer only small variations. Large variations become possible only if $c_1 < 3/5$, because the LK-resonance is then possible.

If the system is in LK-resonance, the secular e and i vary periodically; the maximum eccentricity is achieved at $i = 0$, and the maximum inclination at $e = 0$. The maximum values of eccentricity and inclination obtainable during these variations depend on the value of c_1. For instance, $e_{\rm max} = 0.87$, 0.98, and $i_{\rm max} = 60°$, 78°, if $c_1 = 0.5$, 0.2, respectively (Kozai 2012). For the main-belt asteroids, the periods of such variations are typically of the order of a few thousand years; on this reason, the secular variations cannot be detected directly for this kind of objects; they are studied numerically (by numerical integrations) and analytically.

[5] Note that when we speak here on the constancy of any element, the long-term (average) behaviour in the double-averaged problem is implied. In the single-averaged problem (and, of course, in the original non-averaged problem), the solution oscillates around the mean values given by the solution of the double-averaged problem.

[6] The analogous well-known separatrix of the mathematical pendulum is illustrated in Fig. 4.5.

3.2.4 The Lidov-Kozai Diagrams

Using the LK integrals c_1 and c_2, one can visualize patterns of the secular dynamics by constructing suitable diagrams, representing contour plots of the solutions (level curves of the Hamiltonian). Examples of such diagrams were provided already by Kozai (1962) and Lidov (1963b).

In particular, Kozai (1962) proposed a convenient technique to analyze the qualitative properties of the secular effects: he constructed phase portraits, characterizing the secular evolution of the eccentricity and the argument of pericenter for various initial conditions. Taking into account that the corresponding phase trajectories lie on the level curves of the LK-Hamiltonian, the trajectories can be drawn without integration of the motion equations. The topology of the phase portraits depends essentially on the norm of the vertical component of the particle's orbital angular momentum.

As we know already from the preceding subsection, at its certain value, a bifurcation occurs: whereas for the norm's greater values the argument of pericenter always circulates, for its smaller values an equilibrium point appears, accompanied with the trajectories (around the point), corresponding to libration of the argument of pericenter. This libration island is nothing but the famous *Lidov-Kozai resonance*.

The level curves in the (ω, e) plane are constructed using the relation

$$c_2(\omega, e, c_1) = e^2 \left[\frac{2}{5} - \left(1 - \frac{c_1}{1 - e^2} \right) \sin^2 \omega \right] = \text{const}, \tag{3.38}$$

easily derivable from expressions (3.35) and (3.36). Solving the equation $c_2(\omega, e, c_1) = \text{const}$ on a set of various values of constant c_2 (subject to the inequality $-3/5 \leq c_2 \leq -2/5$), one can visualize the global dynamical behaviour of the system by constructing the corresponding curves in the (ω, e) plane, for one and the same value of c_1.

Using such plots, Kozai (1962) represented graphically the secular dynamics of two asteroids, (1036) Ganymed and (1373) Cincinnati. Ganymed is a NEO (Near-Earth Object) belonging to the Amor group, and Cincinnati is an outer main-belt asteroid. Orbital data for them are presented in Table 7.1; note high values of the inclination and eccentricity. According to the contour plots built by Kozai, (1373) Cincinnati is inside the LK-resonance, whereas (1036) Ganymed is not.

A vivid example (a strictly model one) of a pronounced LK-resonant pattern in the (ω, x) plane, where $x = 1 - e^2$, is given in Fig. 3.2, for $c_1 = (1 - e^2)\cos^2 i = 0.25$. Such contour plots are extensively used now in studies of various astrophysical systems, in particular, in exoplanetary studies. In Fig. 3.3, the contour plot for the same value of c_1 as in Fig. 3.2 is shown as built by Holman et al. (1997) to describe possible secular dynamics of an exoplanet orbiting one of the components of the double star 16 Cyg AB. In Fig. 3.3, a curve given by a direct numerical integration of the non-averaged equations of motion is superimposed on the contour plot. The initial conditions for this integration were chosen to be near the separatrix of the

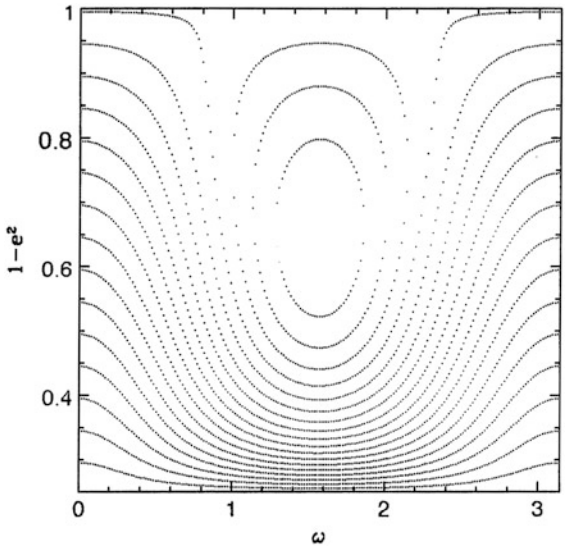

Fig. 3.2 Integral curves at $c_1 = 0.25$ (Figure 3 from Malhotra (2012). With permission from UNESCO-Encyclopedia of Life Support Systems (EOLSS). ©UNESCO-Encyclopedia of Life Support Systems (EOLSS))

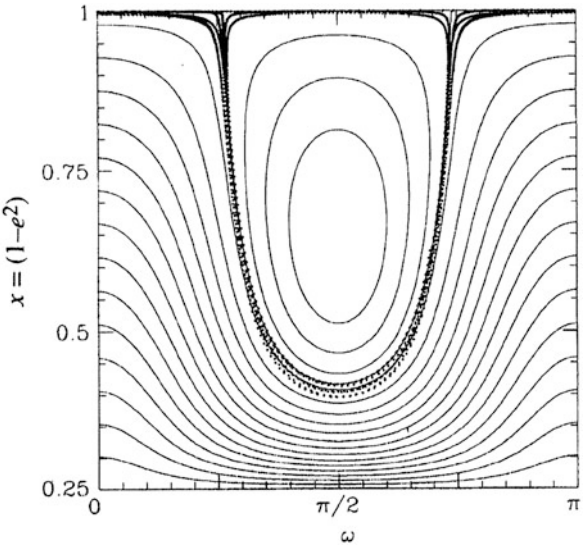

Fig. 3.3 Integral curves at $c_1 = 0.25$, with the chaotic separatrix superimposed; see text for details (Figure 3 from Holman et al. (1997). With permission from Nature Publishing Group)

LK-resonance; therefore, the motion is chaotic and the resulting curve on the graph is irregular. Details on the possible dynamics of planet 16 Cyg Bb are given in Sect. 8.3.

Sometimes, instead of using the Cartesian frame (ω, e) (or, say, (ω, x)), it is more convenient to present the level curves in the polar coordinates, e (or x) as the radial one, and ω as the angular one, thus setting $e\cos\omega$ and $e\sin\omega$ as the Cartesian axes (see, e.g., Broucke 2003; Prokhorenko 2002a,b). We will provide examples of such diagrams further on, when discussing applications.

3.2.5 *The Solution in the Jacobi Elliptic Functions*

The integration of the averaged equations of motion by quadrature requires application of elliptic functions. Already in 1962 Kozai demonstrated that the solution could be found via Weierstrass elliptic functions. In 1968, a partial solution for all required elements except Ω, i.e., for elements e, i, and ω (with the initial condition $\omega_0 = 0, \pm\pi/2$), was explicitly expressed in the Jacobi elliptic functions by Lidov's disciple Yu. F. Gordeeva (1968). The task was completed by Vashkovyak (1999) and Kinoshita and Nakai (1999, 2007), who gave the full explicit elegant solution in the Jacobi elliptic functions.

In this section, we describe how this general solution is obtained, according to Kinoshita and Nakai (2007). This general solution is valid for any initial values of the eccentricity, inclination, and argument of pericenter of the perturbed particle.

In terms of the Delaunay variables (2.15), the averaged Hamiltonian, as we know from Sect. 3.2.1, is a function of three Delaunay momenta and only one angle, ω:

$$\mathcal{H} = \mathcal{H}(L, G, H, \omega), \tag{3.39}$$

see Equation (3.25). Momenta L and H are constant, but G is not. Integral (3.23) has the form

$$c_1 = (H/L)^2 = (1 - e^2)\cos^2 i. \tag{3.40}$$

In what follows, it is used as a parameter. The non-indexed elements a, e, etc., refer to the test particle, as usual.

Kinoshita and Nakai (2007) take the averaged Hamiltonian in the form

$$\mathcal{H} = \beta[(2 + 3e^2)(3\cos^2 i - 1) + 15e^2 \sin^2 i \cos 2\omega], \tag{3.41}$$

where

$$\beta = \frac{m_{\text{pert}}}{16(m_0 + m_{\text{pert}})} n_{\text{pert}}^2 a_{\text{pert}}^2 (1 - e_{\text{pert}}^2)^{-3/2}, \tag{3.42}$$

m_0 and m_{pert} are the masses of the primary and the perturber, a_{pert} and e_{pert} are the semimajor axis and the eccentricity of the perturber, n_{pert} is its mean motion.

Integral (3.24) has the form

$$c_2 = e^2 \left(\frac{2}{5} - \sin^2 i \sin^2 \omega \right). \tag{3.43}$$

On the separatrix, $c_2 = 0$ and $\mathcal{H} = \mathcal{H}(e = 0) = 2\beta(3c_1 - 1)$. As explained in Sect. 3.2.3, the motion is libration or circulation according to the values of c_1 and c_2: if $c_1 > 3/5$, then the motion is circulation; if $c_1 < 3/5$ and $c_2 < 0$, then the motion is libration; if $c_1 < 3/5$ and $c_2 > 0$, then the motion is circulation.

Hamiltonian (3.41) is equivalent to Hamiltonian (3.21), except for the constant coefficient β, in which a dependence on the possible (small) eccentricity of the perturber is taken into account. Therefore, this Hamiltonian is valid, in some approximation, in the elliptic R3BP.[7] The remainder that is ignored in Hamiltonian (3.41) is of the order (in the ratio to the main term) $\sim e e_{\rm pert} a/a_{\rm pert}$, if $e_{\rm pert} \neq 0$, or $\sim (a/a_{\rm pert})^2$, if $e_{\rm pert} = 0$.

The equations for the variables $x \equiv 1 - e^2$ and ω are defined by Hamiltonian (3.41). They are given by

$$\frac{{\rm d}\sqrt{x}}{{\rm d}t} = \frac{15}{8}(x-1)\sin^2 i \sin 2\omega, \tag{3.44}$$

$$\frac{{\rm d}\omega}{{\rm d}t} = -\frac{3}{8}x^{-1/2}\left[x - 5\cos^2 i - 5(x - \cos^2 i)\cos 2\omega\right], \tag{3.45}$$

where the original system's time τ has been normalized, making it unitless: $t = \gamma\tau$,

$$\gamma = \frac{m_{\rm pert}}{(m_0 + m_{\rm pert})}\frac{n_{\rm pert}^2}{n}(1 - e_{\rm pert}^2)^{-3/2}. \tag{3.46}$$

The solution can be found by expressing ω through c_1 and x using the energy constant (3.41), and then substituting the obtained expression for ω in Equation (3.44); thus, Equation (3.44) is reduced to

$$\frac{{\rm d}x}{{\rm d}t} = -3^{3/2}2^{-1/2}\left[(x - x_1)(x - x_2)(x - x_3)\right]^{1/2}, \tag{3.47}$$

where

$$x_1 = \frac{\alpha}{6} - \frac{1}{6}(\alpha^2 - 60c_1), \tag{3.48}$$

$$x_2 = \frac{\alpha}{6} + \frac{1}{6}(\alpha^2 - 60c_1), \tag{3.49}$$

[7] Note that the weakly elliptic R3BP was considered already in the pioneering work by Lidov (1961).

$$x_3 = \frac{1}{4}\left[5 + 5c_1 - \frac{5c_1}{x_0} - x_0 - 5(1-x_0)\left(1 - \frac{c_1}{x_0}\right)\cos 2\omega_0\right], \tag{3.50}$$

$$\alpha = \frac{1}{2}\left[5 + 5c_1 + \frac{5c_1}{x_0} + x_0 + 5(1-x_0)\left(1 - \frac{c_1}{x_0}\right)\cos 2\omega_0\right], \tag{3.51}$$

where $x_0 = 1-e_0^2$; $c_1 = (1-e_0^2)\cos^2 i_0$; the zero subscripts designate that the initial value of a variable is taken: e_0, i_0, and ω_0 are the initial values of the eccentricity, inclination, and argument of pericenter.

Once a solution for x is found, that for ω is given by

$$\sin^2\omega = \frac{2x(x_3 - x)}{5(1-x)(x-c_1)} \tag{3.52}$$

or

$$\cos^2\omega = \frac{3(x_2 - x)(x - x_1)}{5(1-x)(x-c_1)}. \tag{3.53}$$

Defining the quantities

$$x_{\min} = \min\{x_1, x_2, x_3\}, \tag{3.54}$$

$$x_{\text{med}} = \text{med}\{x_1, x_2, x_3\}, \tag{3.55}$$

$$x_{\max} = \max\{x_1, x_2, x_3\} \tag{3.56}$$

(as in Gordeeva 1968), one can write down an explicit formula for x, following from Equation (3.47) by definition of the Jacobi elliptic function cn:

$$x = x_{\text{med}} + (x_{\min} - x_{\text{med}})\,\text{cn}^2\theta, \tag{3.57}$$

where

$$\theta = \frac{2}{\pi}\left(f_\omega t + \omega_0 + \frac{\pi}{2}\right)K(k), \tag{3.58}$$

$$f_\omega = \frac{3^{3/2}\pi}{2^{5/2}K(k)}(x_{\max} - x_{\min})^{1/2}\gamma. \tag{3.59}$$

Here $K(k)$ is the complete elliptic integral of the first kind:

$$K(k) = \int_0^{\pi/2} \frac{\mathrm{d}\theta}{(1 - k^2\sin^2\theta)^{1/2}}, \tag{3.60}$$

and modulus k is given by

$$k^2 = \frac{x_{\text{med}} - x_{\text{min}}}{x_{\text{max}} - x_{\text{min}}}. \tag{3.61}$$

From the solution, the minimum and maximum values of the eccentricity can be determined, which correspond, respectively, to the maximum and minimum values of the inclination. These extrema are given by

$$e_{\text{min}} = (1 - x_{\text{med}})^{1/2}, \quad e_{\text{max}} = (1 - x_{\text{min}})^{1/2}, \tag{3.62}$$

$$i_{\text{min}} = \arccos(c_1/x_{\text{min}})^{1/2}, \quad i_{\text{max}} = \arccos(c_1/x_{\text{med}})^{1/2}. \tag{3.63}$$

The elements e, i, and ω vary with the periods

$$P_e = \frac{\pi}{f_\omega}, \quad P_i = \frac{\pi}{f_\omega}, \quad P_\omega = \frac{2\pi}{f_\omega}, \tag{3.64}$$

where f_ω is given by formula (3.59).

These are nothing but the *periods of LK-oscillations*.

The equation for the longitude of the ascending node is given by a Hamilton's equation, defined by Hamiltonian (3.41) expressed through the Delaunay variables. The resulting equation is analogous to Equation (3.28), and has the form

$$\frac{\mathrm{d}\Omega}{\mathrm{d}t} = \frac{3}{4}\gamma c_1^{1/2}\left(1 - 2\frac{x_3 - c_1}{x - c_1}\right), \tag{3.65}$$

Its solution can be directly expressed through complete and incomplete elliptic integrals of the first and third kinds (Vashkovyak 1999), or it can be found in the form of a Fourier expansion (Kinoshita and Nakai 1999). In the latter approach, one has

$$\Omega = f_\Omega t + \Omega_0 + \sum_{m=1}^{\infty} b_m \sin 2m\omega, \tag{3.66}$$

where

$$f_\Omega = \frac{3}{4}\gamma c_1^{1/2}\left(1 - 2\frac{x_3 - c_1}{x_{\text{max}} - c_1}\right) - \varepsilon\Lambda_0(\xi, k) f_\omega, \tag{3.67}$$

and

$$\Lambda_0(\xi, k) = \frac{2}{\pi}(EF(\xi, k') + KE(\xi, k') - KF(\xi, k')) \tag{3.68}$$

is the Heuman Lambda function; $F(\xi, k')$ is the incomplete elliptic integral of the first kind; E and $E(\xi, k')$ are, respectively, the complete and incomplete elliptic integral of the second kind; $k' = \left(1 - k^2\right)^{1/2}$, and

$$\sin \xi = \left(\frac{x_{\max} - x_{\min}}{x_{\max} - c_1} \right)^{1/2}. \tag{3.69}$$

The quantity ε is given by

$$\varepsilon = \begin{cases} 1, & \text{if } 0 < i < \frac{\pi}{2}, \\ -1, & \text{if } \frac{\pi}{2} < i < \pi. \end{cases} \tag{3.70}$$

The Fourier coefficients are given by

$$b_m = -\frac{2(-q)^m}{m(1 - q^{2m})} \sinh \frac{m\pi F(\xi, k')}{K}, \tag{3.71}$$

where the Jacobi nome, according to Abramowitz and Stegun (1970), is given by

$$q = \exp\left(-\pi \frac{K'(k)}{K(k)} \right), \tag{3.72}$$

$$K'(k) = \int_0^{\pi/2} \frac{\mathrm{d}\theta}{[1 - (1 - k^2) \sin^2 \theta]^{1/2}}. \tag{3.73}$$

The period of LK-oscillations of the argument of ascending node is given by

$$P_\Omega = \frac{2\pi}{f_\Omega}, \tag{3.74}$$

where f_Ω is given by formula (3.67).

This completes the analytical solution in the version of Kinoshita and Nakai (2007).

Kinoshita and Nakai (2007) checked its accuracy by a comparison with direct numerical integrations of the original non-averaged equations of motion in the elliptic R3BP. The integrations were performed for an asteroid and a planetary satellite, namely, a main-belt asteroid (3040) Kozai and an irregular Neptunian satellite Laomedeia NXII. (3040) Kozai orbits the Sun and is perturbed mostly by Jupiter, whereas Laomedeia orbits Neptune and is perturbed mostly by the Sun.

Orbital data on (3040) Kozai and Laomedeia are given in Tables 7.1 and 5.4, respectively. (3040) Kozai is a main-belt asteroid with the current orbital elements $a = 1.84$ AU, $e = 0.20$, $i = 47°$. Laomedeia, also called Neptune XII or S/2002 N3, is a prograde irregular satellite of Neptune with $a = 24$ mln km, $e = 0.40$, $i = 34°$. Thus, the orbits of both objects are strongly inclined with respect to the reference

planes, defined by the orbital planes of the perturbers. (In fact, the reference planes, from which the inclinations are measured, are approximately the ecliptic plane in both cases.)

As follows from both the analytical and numerical solutions, (3040) Kozai resides in LK-resonance (ω librates), and Laomedeia does not (ω circulates), though it is close to LK-resonance.

The osculating elements were used in both integrations, but the results were averaged to provide a better comparison with the analytical solution. Nevertheless, in both cases, the averaging-out of the short-periodic terms induced differences between the osculating and mean elements, thus causing inevitable differences between the analytical and numerical solutions. This factor dominated the (small) inaccuracy of the analytical solution in case of Laomedeia.

In case of (3040) Kozai, another circumstance produced a greater inaccuracy. Indeed, the ratio of the semimajor axes of the asteroid and the perturber are not at all small for (3040) Kozai: $a/a_{\text{Jupiter}} \simeq 0.35$, and on this reason the neglected terms in the perturbing function are not small enough. Therefore, the analytical solution is not so much accurate, as in case of Laomedeia. For Laomedeia, the ratio of the semimajor axes of the satellite and the perturber is ≈ 70 times less; therefore, the neglected terms are indeed small.

Despite these inevitable consequences of approximation, the analytical solution provides a rather good qualitative description of the dynamical behaviour for both (3040) Kozai and Laomedeia.

3.3 LKE-Preventing Phenomena

Let us discuss how the LKE can be suppressed in various dynamical situations. Indeed, if an additional perturbation dominates over the LK-term in the Hamiltonian of the motion, then the LKE may disappear (Lidov 1963b; Morbidelli 2002).

Such suppression explains, e.g., the stable existence of the *regular* Uranian satellites, considered already in 1963 by Lidov (1963b). The suppression "agent" here is the satellites' orbital precession forced by the Uranus oblateness and the moons' mutual perturbations.

The LKE suppression phenomena may have various origins. An example is presented by the stability of our Solar system notwithstanding the *Galactic tide*. Indeed, the planetary orbits in the Solar system are subject to long-term perturbations due to the Galactic tide; and, being inclined by $\sim 60^\circ$ with respect to the Galactic plane, the Solar system might seem to be vulnerable to destabilization by the LKE. In reality, luckily for us, the LKE is suppressed by the precession of the planetary orbits due to their mutual perturbations. Only at the distance of about a hundred thousand AU (the radius of the Oort cloud) from the Sun the LKE becomes operational (Matese and Whitman 1992; Morbidelli 2002).

Another vivid example is provided by the fact that in some compact binaries, subject to a perturbation from a distant companion star, the LKE-suppressing mechanism is due to the relativistic precession of the inner binary (Fabrycky and Tremaine 2007).

Thus, an assessment of the LKE effectiveness in real celestial-mechanical systems often needs taking into account possible interfering perturbations, – sometimes rather weak, because the LKE acts on long timescales.

To assess the LKE effectiveness analytically, the most easy way is to compare the timescale of the LKE in a given problem with the period of the orbital precession caused by a suppressing mechanism that may be in action. There is a number of suppressing mechanisms. The most ubiquitous are: (1) gravitational perturbations from other (than the secondary) bodies orbiting the primary; (2) primary's or tertiary's non-sphericity implying non-zero quadrupole moments; (3) general relativity. The second one subdivides in two important factors: (2*a*) oblateness of the primary's figure, due to rotation; (2*b*) tidal interaction between the primary and the tertiary, implying deformations of their figures. Historically, it is just case 2*a* that was first recovered as a mechanism suppressing the LKE (Lidov 1963b).

Of course, all the suppressing mechanisms may act in concert. Generally, the perturbations are small, that is why the total rate of precession of the line of apsides (the total rate of change of the longitude of pericenter) can be written as a linear sum:

$$\dot{\varpi}_{\rm sum} = \dot{\varpi}_{(1)} + \dot{\varpi}_{(2a)} + \dot{\varpi}_{(2b)} + \dot{\varpi}_{(3)}. \tag{3.75}$$

An analogous formula can be written for the total rate of change of the longitude of ascending node. For our purposes (comparison of the precession rates) it is enough to consider the rates of change of the longitude of pericenter.

3.3.1 Perturbations by Additional Orbiting Bodies

Suppose one has a system demonstrating the LKE; then, if an additional orbiting body with non-zero mass is introduced in the system, the precession caused by the perturbation from the introduced body may suppress the otherwise present LKE. The suppression of this kind is possible in N-body systems with $N \geq 4$.

A famous example of the orbital precession caused by orbiting bodies is given by the orbital precession of Mercury. The rate of Mercury's apsidal precession due to the perturbations from all other planets is equal to $532''$ per century; the general relativity adds $43''$ per century, whereas the Solar oblateness and tidal effects are negligible (see, e.g. Clemence 1947). Thus, in Mercury's precession, the contribution of the planetary perturbations is the dominant one.

The basic expressions describing the secular evolution in the circumbinary and circumcomponent planar cases are given in Chap. 8. The formula for the precession

rate is individual in each of these two cases. It is given by

$$\dot{\varpi} = \frac{3\pi}{2} \frac{m_0 m_1}{(m_0 + m_1)^{3/2}} \frac{a_\mathrm{b}^2}{a^{7/2}} \left(1 + \frac{3}{2} e_\mathrm{b}^2\right) \tag{3.76}$$

in the circumbinary case (here the barycentric frame is adopted), and by

$$\dot{\varpi} = \frac{3\pi}{2} \frac{m_1}{m_0^{1/2}} \frac{a^{3/2}}{a_\mathrm{b}^3} \left(1 - e_\mathrm{b}^2\right)^{-3/2} \tag{3.77}$$

in the circumcomponent case (here an astrocentric frame is adopted); m_0 and m_1 are the masses of the binary components (we set $m_0 \geq m_1$), a_b is the binary semimajor axis, e_b is the binary eccentricity, a is the semimajor axis of the particle's orbit. The masses are measured in Solar units, distances in astronomical units (AU), and time in years. Thus, the gravitational constant $\mathcal{G}$ is equal to $4\pi^2$. The formulas are derived in the hierarchical setting of the restricted three-body problem.

Formula (3.77) can be applied to estimate the rate of Mercury's precession caused by other planets; it provides rather good results for each planet contribution (which are listed, e.g., in Clemence 1947), except for the contribution of Venus, because the configuration Sun–Mercury–Venus is rather far from hierarchical.

3.3.2 *Primary's Oblateness*

Let us consider the orbital precession of a satellite orbiting an oblate massive central body (a planet). In our analysis we follow an approach adopted by Roy (1988) and Murray and Dermott (1999). First of all, let us introduce orthogonal and spherical coordinate frames for a satellite of a planet, as depicted in Fig. 3.4: x, y, z are the Cartesian coordinates; r, λ, φ are the spherical coordinates: satellite's radial distance, longitude, and latitude, respectively.

The axisymmetric gravitational potential of a non-spherical body (a primary) is given by the expression

$$\mathcal{V} = -\frac{\mathcal{G} m_\mathrm{p}}{r} \left[1 - \sum_{i=2}^{\infty} J_i \left(\frac{R_\mathrm{p}}{r}\right)^i P_i(\sin\varphi)\right], \tag{3.78}$$

where $\mathcal{G}$ is the gravitational constant, m_p and R_p are the mass and mean radius of the planet, P_i are the Legendre polynomials of degree i, J_i are the so-called zonal harmonics, which characterize the oblateness. The quantities J_i are unitless. Odd harmonics J_{2j+1} ($j = 1, 2, \ldots$) are generally small for planets (though the Earth has $J_3 \approx 1.5 J_4$). The first two even harmonics J_2 and J_4, measured for the planets of our Solar system, are listed in Table 5.1.

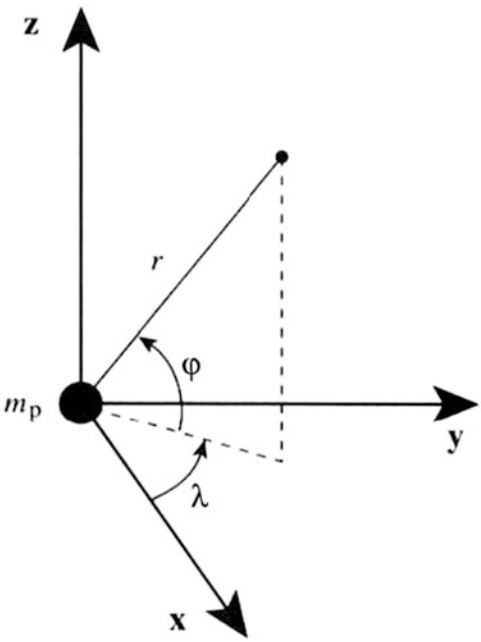

Fig. 3.4 The Cartesian and spherical coordinate frames for a planetary satellite: x, y, z are the Cartesian coordinates, and r, λ, φ are the radial distance, longitude, and latitude of the satellite (Figure 6.6 from Murray and Dermott (1999). With permission from Cambridge University Press)

For a satellite moving in an orbit with semimajor axis a around a spherical central body ($J_i = 0, i = 2, 3, \ldots$), potential (3.78) reduces to the potential of a gravitating point, and the mean motion is given by the expression $n_0 = (\mathcal{G}m_\mathrm{p}/a^3)^{1/2}$, following from Kepler's third law. For a satellite moving around a planet with $J_2 \neq 0$ (an oblate planet), the mean motion is given by

$$n = n_0 \left[1 + \frac{3}{2} J_2 \left(\frac{R_\mathrm{p}}{a} \right)^2 \right]^{1/2} \tag{3.79}$$

(Murray and Dermott 1999). Thus, generally, $n > n_0$ for a fixed a.

Let us adopt an approximate expression for the perturbing function, truncated at the lowest order of expansion in R_p/r:

$$\mathcal{R} = -\frac{\mathcal{G}m_\mathrm{p}}{r} \cdot J_2 \left(\frac{R_\mathrm{p}}{r} \right)^2 P_2(\sin\varphi), \tag{3.80}$$

where

$$P_2(\sin\varphi) = \frac{1}{2}(3\sin^2\varphi - 1). \tag{3.81}$$

Considering Fig. 3.4, one has

$$\begin{pmatrix} x \\ y \\ z \end{pmatrix} = r \begin{pmatrix} \cos\Omega\cos(\omega+f) - \sin\Omega\sin(\omega+f)\cos i \\ \sin\Omega\cos(\omega+f) + \cos\Omega\sin(\omega+f)\cos i \\ \sin(\omega+f)\sin i \end{pmatrix}, \tag{3.82}$$

where i is the inclination, f is the true anomaly, and ω is the argument of pericenter. Therefore, the latitude φ is given by the equation

$$\sin\varphi = \sin i \sin(f+\omega). \tag{3.83}$$

Then, one can (1) substitute $r = a(1-e^2)/(1+e\cos f)$ in $\mathcal{R}$, given by expression (3.80); (2) represent $\sin f$ and $\cos f$ as the power series in the mean anomaly M; and, finally, (3) average $\mathcal{R}$ over M ($0 \le M \le 2\pi$). This gives the averaged $\mathcal{R}$, up to the second order in e and $\sin i$ and in the lowest order of expansion in R_p/a:

$$\langle\mathcal{R}\rangle = \frac{3}{4} J_2 R_\mathrm{p}^2 n^2 (e^2 - \sin^2 i). \tag{3.84}$$

Taking the Lagrange planetary equations (provided, e.g., in Subbotin 1968, or Murray and Dermott 1999) for the longitude of pericenter ϖ and for the longitude of ascending node Ω, and using formula (3.84) for the perturbing function and formula (3.79), one has finally in the lowest order of expansion in R_p/a:

$$\dot{\varpi} = \frac{3}{2} J_2 n_0 \left(\frac{R_\mathrm{p}}{a}\right)^2, \tag{3.85}$$

$$\dot{\Omega} = -\frac{3}{2} J_2 n_0 \left(\frac{R_\mathrm{p}}{a}\right)^2. \tag{3.86}$$

We see that $\dot{\varpi} = -\dot{\Omega}$ in this approximation.

3.3.3 Tides

The tidal phenomena are important in tight astrophysical binaries, such as tight binary stars, binary asteroids, star–planet systems, first of all the systems with "hot Jupiters". For the tight stellar binaries also a mutual mass transport may play a significant role, apart from the tidal deformations. For a star–planet system, a general picture of the tidal precession is given by Ragozzine and Wolf (2009), for a binary asteroid by Perets and Naoz (2009) and Fang and Margot (2012). An introduction to the celestial-mechanical theory of tides, including definitions of the

effective dissipation parameter Q, the Love number, etc., can be found in Murray and Dermott (1999). The tidal precession is a complex phenomenon, that is why we consider only basic results here, appropriate for exoplanetary applications discussed in the book further on.

In a star–planet system, the tidal bulge raised on the planet is always aligned almost exactly towards the star: the lag angle $\sim 1/Q$, where the effective dissipation parameter $Q \gg 1$ (e.g., for the giant planets one has $Q \gtrsim 10^5$). On the other hand, the height of the bulge strongly varies with the "star–planet" distance, sharply falling with increasing the distance. This inhibits any description based on a single constant value of the J_2 harmonic. For the tidal bulge raised on the star, the situation is the same; however, the bulge on the planet is most important for the precession. Taking into account the dependence of the bulge size on the "star–planet" distance allows one to estimate the tidal precession rate with a satisfactory accuracy (Ragozzine and Wolf 2009; Sterne 1939).

According to Sterne (1939) and Eggleton and Kiseleva-Eggleton (2001), the rate of the apsidal precession due to the tidal bulges, raised on both the primary and the secondary ("star" and "planet"), is given by

$$\dot{\varpi}_{\rm tidal} = \dot{\varpi}_{\rm tidal,\,0} + \dot{\varpi}_{\rm tidal,\,1} =$$

$$= \frac{15}{2} k_{2,0} \left(\frac{R_0}{a}\right)^5 \frac{m_1}{m_0} f(e) n + \frac{15}{2} k_{2,1} \left(\frac{R_1}{a}\right)^5 \frac{m_0}{m_1} f(e) n, \tag{3.87}$$

where

$$f(e) = (1-e^2)^{-5} \left(1 + \frac{3}{2}e^2 + \frac{1}{8}e^4\right) \approx 1 + \frac{13}{2}e^2 + \frac{181}{8}e^4 + \ldots. \tag{3.88}$$

The subscripts 0 and 1 refer to the primary and the secondary, respectively; m, R, and k_2, are the masses, mean radii, and Love numbers of the bodies; n, a, and e are, respectively, the mean motion, size and eccentricity of the binary.

The Love number k_2 is a unitless quantity that characterizes an effect of an applied potential on the gravity field of the planetary interiors. It can be calculated, given the interior density distribution (e.g. Sterne 1939). If the density rises towards the center, i.e., the mass is concentrated to the core, then the k_2 values are small ($k_2 \ll 1$). In this case, the gravity field is mostly unaffected by the masses located closer to the surface of the object. This is typical for the stars: e.g., the Solar-type stars have $k_2 \sim 0.03$ (Claret 1995).

Planets, especially rocky planets, are different in this respect: their gravity fields are strongly affected by the distortions of mass distributions near their surfaces. The weaker the object is condensed towards its center, the greater is its k_2. A spherical object with uniform density has $k_2 = 3/2$; this is the maximum value for the Love number. The gas giants Jupiter and Saturn have $k_2 \simeq 0.49$ and 0.32, respectively, indicating the presence of relatively massive cores.

The size of the tidal bulge is directly proportional to the mass of the body that raises the tide, and the tide on the planet is dominant in determining the precession rate. The ratio of the rates induced by the secondary and the primary is given by the formula

$$\frac{\dot{\varpi}_{\mathrm{tidal},\,1}}{\dot{\varpi}_{\mathrm{tidal},0}} = \frac{k_{2,\,1}}{k_{2,0}} \left(\frac{R_1}{R_0}\right)^5 \left(\frac{m_0}{m_1}\right)^2. \tag{3.89}$$

For a typical "star–planet" system this ratio is estimated to be $\simeq$ 100 (Ragozzine and Wolf 2009).

3.3.4 General Relativity

Einstein's explanation of the "anomalous" precession of the pericenter of Mercury's orbit was one of the major successes of the theory of general relativity. As in the case with Mercury, general relativity can contribute much to the apsidal precession of exoplanets, because many of them (especially, the "hot Jupiters") move in tight orbits. The rate of the relativistic precession (in radians per planetary orbital revolution) is directly proportional to the ratio of the gravitational radius R_{g} of the parent star and the pericentric distance q of the planetary orbit. Einstein's formula for the apsidal precession rate is

$$\dot{\varpi}_{\mathrm{GR}} = \frac{6\pi\mathcal{G}m_0}{c^2 a(1-e^2)} = \frac{6\pi R_{\mathrm{g}}}{a(1-e^2)} = \frac{6\pi R_{\mathrm{g}}}{q(1+e)}, \tag{3.90}$$

where $\mathcal{G}$ is the gravitational constant, m_0 and $R_{\mathrm{g}} = \mathcal{G}m_0 c^{-2}$ are the mass and the gravitational radius of the body around which the particle orbits, c is the speed of light, e is the eccentricity of the planetary orbit (see, e.g. Clemence 1947).

As follows from Equation (3.90), the smaller is the pericentric distance $q = a(1-e)$, the more rapid is the precession. For "hot Jupiters", $\dot{\varpi}_{\mathrm{GR}}$ can reach rather large values, exceeding the value for Mercury by orders of magnitude.

The rate of Mercury's apsidal precession due to the perturbations from all other planets is equal to 532″ per century; the general relativity adds 43″ per century (see, e.g. Clemence 1947). The planetary contributions to the orbital precession of Mercury (the exact values, as cited in Clemence (1947), and the values given by Heppenheimer's formula (3.77)) are listed in Table 3.1. Note that the only serious differences of the analytical estimates from the exact numerical ones take place for Venus and Earth, because the hierarchical approximation, in which formula (3.77) is valid, breaks down for them.

Table 3.1 Contributions to the advance of the perihelion of Mercury, in arcseconds per century

Planet	Exact value (Clemence 1947)	Value given by Eq. (3.77)
Venus	277.86 ± 0.68	151.42
Earth	90.04 ± 0.08	70.34
Mars	2.54	2.164
Jupiter	158.58	159.27
Saturn	7.30 ± 0.01	7.707
Uranus	0.141	0.1455
Neptune	0.042	0.0446

3.3.5 The Orbital Precession in Total

The four giant planets of our Solar system rotate very fast, all of them have periods of axial rotation of the order of 10 h. On this reason their figures are significantly oblate, especially in the cases of Jupiter and Saturn; see Table 5.1. The rotational oblateness of the planets dominates over other effects determining the apsidal precession of the satellites of these planets.

The "hot Jupiters", apart from the fact that they move close to their parent stars, have another serious distinction from the giant planets of our Solar system: their axial rotation is drastically slower. At close distances to the parent stars, the tidal slowing-down of the rotation leads to its synchronization with the orbital motion. In the synchronous state, one and the same side of a planet is exposed to the parent star, analogously to the synchronous state of the Moon with respect to the Earth. (Note that the tidal effect sharply rises with decreasing the orbital semimajor axis.) Thus, the rotational oblateness of the parent planets contributes little to the total apsidal precession of such planets. Instead, the tides dominate over all other contributions. *Very hot Jupiters* (the giant exoplanets with semimajor axes $a \lesssim 0.025\,\mathrm{AU} \sim 6$ stellar radii) are expected to have the tides on the planets that induce the orbital precession with the rate up to $\approx 20°$ per year, as in the case of WASP-12b (Ragozzine and Wolf 2009).

For the hot Jupiters, the general relativity is the second most important contribution to the apsidal precession. Generally, it evokes the precession by an order of magnitude slower than that evoked by the planetary tidal bulge (Ragozzine and Wolf 2009).

If the contributions to the total precession rate are all small, the total rate can be calculated as a linear sum of the individual contributions, see Equation (3.75). Comparing the period of the total precessional effect with the period of LK-oscillations, one can judge whether the LKE is suppressed or not.

3.4 Critical Radii

Studying the motion of Jovian satellites, already in 1805 Laplace realized that the choice of a convenient reference plane for defining the orbital inclination of a satellite depends on the size of its orbit (Laplace 1805): near the planet, where perturbations caused by the planet's oblateness dominate, it is pertinent to measure the inclinations with respect to the planet's equatorial plane, whereas far from the planet, where Solar perturbations dominate,—with respect to the planet's ecliptic plane. In intermediate situations, the reference plane is defined as the plane orthogonal to the axis of precession of a satellite's orbit (e.g., Tremaine et al. 2009). Indeed, if a satellite has the orbital semimajor axis large enough, the precession of its orbit is mostly controlled by the Sun; conversely, if the orbit size is small, it is controlled by the parent planet's oblateness.

Thus, for the planetary satellites in the low orbits where the perturbations caused by the host planet's oblateness dominate, the Laplace plane is approximately the planet's equatorial plane; for the planetary satellites in the high orbits where the Solar perturbations dominate, the Laplace plane is approximately the planet's ecliptic plane. The transition between these two limits takes place at a radial distance from the planet known as the *Laplace radius*:

$$r_{\mathrm{L}} = \left[J_2 \frac{m_{\mathrm{p}}}{m_{\mathrm{Sun}}} R_{\mathrm{p}}^2 a_{\mathrm{p}}^3 \left(1 - e_{\mathrm{p}}^2\right)^{3/2} \right]^{1/5} \tag{3.91}$$

(Goldreich 1966; Tamayo et al. 2013; Tremaine et al. 2009), where m_{p} and m_{Sun} are the masses of the planet and the Sun, R_{p}, J_2, a_{p}, and e_{p} are the planet's mean radius, second zonal harmonic coefficient, orbital semimajor axis and eccentricity, respectively.

In fact, as follows from its definition, the Laplace radius plays the role of the *critical radius* above which the LKE becomes operational. The notion of critical radius is easily generalized to the cases of other possible perturbations. Indeed, the period of precession induced by any of the known LKE-preventing mechanisms (considered in the preceding section) increases with the distance from the system center (because the cause of precession becomes farther from the particle), whereas the period of LK-oscillations, on the contrary, diminishes (because the perturber becomes closer). Therefore, in each case, a distance from the center exists where the periods become equal. This is just the *critical radius*, above which the LKE becomes operational.

Formula (3.59) gives the exact frequency of LK-oscillations. An approximate frequency is given by the constant factor of Equation (3.32). Equating the LK-frequency sequentially to the frequencies of precession induced by the primary's non-sphericity, tides, or general relativity, one gets equations defining the critical

radius $a = a_{\rm crit}$ in each case:

$$\dot{\omega}_{\rm LK}(a) \approx \dot{\omega}_{\rm obl}(a), \tag{3.92}$$

$$\dot{\omega}_{\rm LK}(a) \approx \dot{\omega}_{\rm tidal}(a), \tag{3.93}$$

$$\dot{\omega}_{\rm LK}(a) \approx \dot{\omega}_{\rm GR}(a). \tag{3.94}$$

Based on Equation (3.92), formula (3.91) can be derived by retaining the leading terms in formulas (3.85) and (3.86), calculating the difference $\dot{\omega} = \dot{\varpi} - \dot{\Omega}$, and equating $\dot{\omega}$ to the LK-frequency, given by Equation (3.32). The same result is achieved by equating $\dot{\varpi}$ to that given by formula (3.77) (note that the unit system should be adjusted in the latter case).

Equations (3.93) and (3.94) define the critical radii for the cases of tidal and general-relativistic perturbations, respectively. To obtain explicit relations, the frequencies given by formulas (3.87) and (3.90) should be substituted in the right-hand sides of the equations.

Apart from the listed perturbations, the LKE can be quenched by perturbations from inner (with respect to the test particle) bodies orbiting the primary. Their effect can be incorporated in formula (3.91) by modifying the value of J_2:

$$J_2' = J_2 + \frac{1}{2R_{\rm p}^2} \sum_{i=1}^{n} \frac{m_i}{m_{\rm p}} a_i^2, \tag{3.95}$$

and by substituting J_2' instead of J_2 in formula (3.91) (Tremaine et al. 2009). Here it is supposed that n satellites move in circular equatorial orbits around the planet; their orbits are much smaller in size than that of the test particle. The physical sense of the formula is that the perturbing satellites are "spread" by averaging along the orbits, thus enhancing the physical oblateness of the central body.

Finishing this Chapter, let us consider a remarkable example of a system where the LKE is suppressed *twice*. This is the satellite system of Pluto. In fact, Pluto and Charon form a central binary of this system: the mass ratio of Charon and Pluto is rather large, $m_1/m_0 = 0.12$. The inclination of the binary's plane, with respect to the plane of the binary's orbit around the Sun, is equal to 119°; therefore, the question immediately arises: why the system is not destabilized by the LKE induced by the Sun? Or, maybe, we observe it in the process of destabilization?

The answer is that the binary's orbital precession induced by the Pluto–Charon tidal interaction dominates over the secular motions induced by the LKE; thus, the LKE is quenched (Michaely et al. 2015). Then, another question is immediate: what about other satellites, Styx, Nix, Kerberos and Hydra, which move in wider orbits coplanar with the central binary? For them, the tidal effect is negligible, because it sharply diminishes with increasing the distance from the system's center. The answer, in its turn, is that the LKE-quenching precession is still induced for them, but by another mechanism,—that conditioned by the non-point-mass gravitational potential of the central binary Pluto–Charon.

In the presence of a central binary, the critical orbital radius above which a satellite cannot survive, due to the LKE, can be calculated by means of formula (3.91), where J_2' is substituted instead of J_2. In formula (3.95), the original J_2 is set to zero, and it is enough to take only Charon in account, i.e., $n = 1$. On similar grounds, Michaely et al. (2015) derived the following formula, which allows one to estimate the critical semimajor axis $a_{\rm crit}$ in such systems:

$$a_{\rm crit} = \left[\frac{3m_1 m_2 \left(1 - e_1^2\right)^{3/2}}{8m_0(m_1 + m_2)\left(1 - e^2\right)^{3/2}} \left(5\cos^2 i - 1\right) \right]^{1/5} \left(a_1^3 a_2^2\right)^{1/5} , \tag{3.96}$$

where m_0 is the mass of the perturber, and $m_1 \geq m_2$ are the two masses comprising the binary orbiting the perturber; a_1 and a_2 are the semimajor axes of the "large" and "small" binaries, respectively (the large binary is formed by the perturber and the barycenter of the small binary); e_1 is the eccentricity of the large binary. The small binary is assumed to be circular, i.e., $e_2 = 0$. The semimajor axis and eccentricity of an outer massless satellite of the small binary are designated by a and e; and i is the inclination of the satellite's orbit with respect to the orbital plane of the small binary. It is assumed that the inclination of the small binary with respect to the large binary is high enough, so that the LK-resonance is potentially present.

In the Sun-perturbed Pluto–Charon system, m_0, m_1, and m_2 are, respectively, the masses of the Sun, Pluto, and Charon; a_1 and a_2 are, respectively, the semimajor axis of Pluto's orbit around the Sun and the semimajor axis of the Pluto–Charon binary; e_1 is the eccentricity of Pluto's orbit around the Sun; and $e_2 = 0$ (the Pluto–Charon binary is almost circular). Substituting the values of all these quantities in formula (3.96), one finds $a_{\rm crit} = 0.004\,\text{AU}$. As Michaely et al. (2015) found out, all satellites of the Pluto–Charon binary lie well within this limit; the most distant one, Hydra, follows an orbit whose size is by an order of magnitude less than $a_{\rm crit}$. On the other hand, the value of $a_{\rm crit}$ is still much smaller than the Hill radius of the Pluto–Charon system.